

A Novel Structure of High Speed OFDM Receiver to Overcome ISI and ICI in Rayleigh Fading Channel

Ashraf Y. Hassan¹ 

Published online: 29 July 2017
© Springer Science+Business Media, LLC 2017

Abstract High-Speed Orthogonal-Frequency-Division-Multiplexing (HS-OFDM) is an OFDM system with high OFDM symbol rate. In HS-OFDM system, the symbol period is comparable with the multipath delay-spread of the channel. No cyclic-prefix is used with HS-OFDM to increase the bandwidth efficiency. HS-OFDM suffers from Inter-Symbol Interference (ISI) and Inter-Carrier Interference (ICI) signals. In this paper, a complete mathematical model of the received HS-OFDM signal with both ISI and ICI interfering signals are represented. A novel receiver that tracks the time-varying channel gain and reduces the effects of the interfering signals, is proposed based on the deduced mathematical model. The new receiver depends on a new arrangement of decision-feedback equalizer, which is designed in frequency domain. The paper illustrates how the taps of the equalizer are calculated, and it calculates the remaining amount of interference after the use of the proposed receiver. The used model of the wireless channel in HS-OFDM system is the frequency-selective channel. It models the outdoor channel in HS-OFDM system.

Keywords Orthogonal frequency division multiplexing · Inter-symbol interference · Inter-carrier interference · Rayleigh fading channel

1 Introduction

OFDM is an advanced modulation technique used in the transmission of data over wireless channel with high data rates. OFDM can be seen as either a modulation technique or a multiplexing technique. OFDM is used in many modern applications such as digital audio and video broadcasting, digital terrestrial multimedia broadcast, wireless local area networks, and some standards of the fourth generation mobile phones. OFDM can support

✉ Ashraf Y. Hassan
Ashraf.Fahmy@bhit.bu.edu.eg

¹ Benha Faculty of Engineering, Benha University, Benha, Egypt

high data rates through parallel transmission of users' symbols over M orthogonal sub-carrier instead of a single carrier.

In the proposed HS-OFDM, the total rate of data transmission is increased by increasing the OFDM symbol rate. However, the data rate is increased by increasing the number of the subcarriers in the conventional OFDM system. Increasing the number of the subcarriers increases the ICI signal, which is not a trivial problem in OFDM systems. On the other hand, the OFDM symbol rate is often smaller than the multipath delay-spread of the channel. This prevents ISI between the transmitted symbols on each OFDM sub-channel. In the proposed HS-OFDM system, the ISI signal exists. The coherent bandwidth of the channel is usually equal to or smaller than the bandwidth of the HS-OFDM sub-channel. This ISI signal can be canceled or reduced by using ISI cancellation techniques. The number of the subcarriers in the proposed HS-OFDM system is smaller than the number of the subcarriers in the conventional OFDM, which supports the same total bit rate. Therefore, the ICI signal in the proposed HS-OFDM is smaller than the ICI in the analogous conventional OFDM. The proposed HS-OFDM system compromises between increasing the OFDM symbol rate and the residual ICI and ISI signals. This paper proposes a receiver structure for the HS-OFDM, which minimizes the ISI and ICI at the input of the detector.

In this paper, the HS-OFDM is studied in macro-cell mobile channel. The macro-cell mobile channel is well modeled as a frequency-selective channel. Its multipath delay-profile is bigger than the transmitted symbol period. Typical values of the multipath delay-spread are $0.5 \mu\text{s}$ for suburban areas and $6 \mu\text{s}$ for urban areas. These values are measured in many sites in Egypt by the communication research group in Benha University.

One of the main reasons to use OFDM is to increase the robustness against frequency-selective fading or narrowband interference. In order to mitigate ISI signal, a cyclic prefix (CP) is usually added to the front of each OFDM symbol [1]. To ensure that the ISI is completely removed, the CP length must be more than or equal to the length of the channel impulse response (CIR). Actually, the CP carries no data and it reduces the bandwidth efficiency.

$$\eta = \frac{1}{BW \cdot (T + T_{cp})} \quad (1)$$

T is the period of the OFDM symbol. T_{cp} is the cyclic prefix period. In order to improve the bandwidth efficiency, the cyclic prefix should be minimized or canceled. In the proposed HS-OFDM, CP is removed. This increases the bandwidth efficiency of the HS-OFDM system. However, the ISI signal is increased because the multipath delay-spread of the channel is longer than the cyclic prefix. Decision-Feedback Equalizer (DFE) is used to reduce the ISI signal. In addition, the random time-varying impulse response of the wireless channel causes signal degradation. Using adaptive techniques in the implementation of the equalizer counteracts the time-varying nature of the channel.

Several methods for designing equalizers have been proposed to reduce or cancel the ISI and ICI presented in OFDM system with insufficient CP. A time-domain linear equalizer aims to shorten the effective length of the Overall Impulse Response (OIR) between the modulator and demodulator. This is done according to a predetermined criterion, such as accumulating the energy of the convolution between the channel and the equalizer in a suitable window [2], or minimizing the average value of signal to interference plus noise ratio SINR for all subcarriers [3] [4], or minimizing the delay-spread of the overall

impulse response [5]. In the second approach, the mean square error MSE between the real CIR and the desired OIR is minimized [6].

On the other hand, a new model for formulating the OFDM signal, noise and interference is developed at the receiver's input [7]. This model is used to design a decision feedback equalizer DFE that is able to remove both ISI and ICI. The feedback path of this DFE receiver is responsible for removing the ISI, while the forward path is used to suppress the ICI as well as demodulating the signal. A zero forcing criterion is used in [7] and the additive noise has been neglected for simplicity. However, when the channel is severely frequency selective, this simplification affects the equalizer performance due to instability.

In [8], the MMSE criterion is used to reduce the problems of ZF equalizer problem. In addition, the previous data symbols that used in the feedback part of the DFE are taken from the output of the error correction decoder instead of the demodulator output to minimize the probability of error on the feedback data path.

In this paper, a mathematical model for the transmitter and the receiver of the proposed HS-OFDM is represented. The received signal model shows the effects of the frequency-selective channel on the HS-OFDM symbol. The mathematical model of the received HS-OFDM signal demonstrates three terms that represent the faded desired symbol, the ISI signal, and the ICI signal. A frequency domain DFE is used to minimize the ISI and ICI signals instead of a time domain equalizers that are used in all previous works. The feedback path in the proposed equalizer will be designed to minimize the ISI and ICI signals simultaneously, however it was used to minimizing the ISI signal in [7, 8]. The proposed receiver removes the ISI signal and the ICI signal from previous symbols first, and then it removes the ICI signal from the current symbols. However, in [7, 8] ICI signal from current symbols are removed first, and then the ISI signal from the previous symbols is removed by the feedback filter.

The feedback path in the proposed receiver is split into two independent feedback filters. The first feedback filter is fed from the previous detected symbols on the same subcarrier and it is responsible for reducing the ISI signal. The second feedback filter is fed from the previous detected symbols on the other subcarriers and it is responsible for reducing the ICI signal. The proposed equalizer cannot remove the ICI from the current symbols on the non-orthogonal subcarriers. Therefore, linear multiuser detection methods are proposed to remove these interfering symbols. The forward path in the proposed equalizer is designed to minimize the flat fading effect on the desired signal and it tracks the time-varying gain of the channel. Different criteria such as MMSE and LS are used in the design of the forward part of the equalizer to test the performance of the system with slow and fast fading cases. Finally, simulations are done to compare the performance of the proposed HS-OFDM system with the conventional OFDM system in Rayleigh fading channel. Some field measurements are also represented.

Section 2 gives a complete mathematical model of the HS-OFDM transmitted signal, the used time-varying channel, and the received HS-OFDM signal at the input of the proposed HS-OFDM receiver. Section 3 exploits the mathematical models in Sect. 2 and it shows the design of the proposed DFE to reduce the effects of the ISI and ICI signals from the previous symbols on all subcarriers. The power of the residual ISI and ICI signals is also calculated. Section 4 gives a proposal of linear multiuser detection methods that can be used to remove or reduce the ICI from the current symbols on non-orthogonal subcarriers. Section 5 shows the simulations of the proposed HS-OFDM system. A comparison between the performance of the conventional OFDM and the proposed HS-OFDM is shown using simulations and field measurements.

2 Mathematical Modeling of the HS-OFDM in Frequency Selective Channel

The presented model in this section shows the effects of the frequency-selective channel on the received HS-OFDM signal. The model illustrates the output signal of the demodulator, which consists of the desired signal, the interfering signals, and the channel noise.

2.1 Transmitted Signal Model

The block diagram of the HS-OFDM system is shown in Fig. 1. It looks like the block diagram of the conventional OFDM system. The differences between the HS-OFDM and the conventional OFDM systems are the rate of the OFDM symbols and the number of the subcarriers. These differences do not change the structure of the block diagram of the whole OFDM system. In Fig. 1, no CP is attached with each symbol of the HS-OFDM system.

The number of subcarriers in the proposed system is M . The transmitted symbols of the m th sub-carrier are represented by Eq. (2).

$$s_m(t) = \sum_{k=0}^{K-1} d_{mk} p_m(t - kT) \quad m = 0, 1, 2, 3, \dots, M - 1 \tag{2}$$

K is the number of HS-OFDM symbols. d_{km} is the k th complex QAM symbol that modulates the m th subcarrier. $p_m(t)$ is the pulse shape of the m th subcarrier. T is the period of the proposed HS-OFDM symbol. The transmitted HS-OFDM symbols with M subcarriers, which are the output of the OFDM modulator (IFFT block), are represented by Eq. (3)

$$s(t) = \sum_{m=0}^{M-1} \sum_{k=0}^{K-1} d_{mk} p_m(t - kT). \tag{3}$$

2.2 Channel Model

We consider a multipath-channel model. The channel is assumed constant during each HS-OFDM symbol, however it is changed randomly from symbol to another. The channel consists of L independent paths. The impulse response of the channel is:

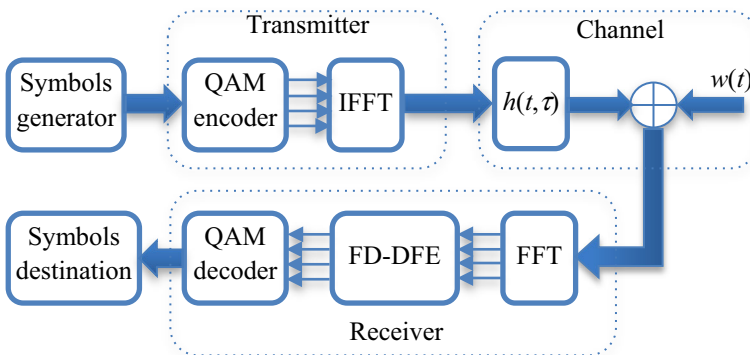


Fig. 1 The block diagram of HS-OFDM system

$$h(t) = \sum_{l=0}^{L-1} \alpha_l(t) e^{j\phi_l(t)} \delta(t - \tau_l) \tag{4}$$

$\alpha_l(t)$ is a time-varying gain. It is a sample function of a Rayleigh random process with a power-delay profile $D(\tau_l)$. $\phi_l(t)$ is a time-varying phase. It is a sample function of a uniform random process. τ_l is the signal delay in the l th path. The delays (τ_l) are distributed uniformly and independently over the delay-spread of the channel. $\alpha_l(t)$ and $\phi_l(t)$ are constant during the period of each HS-OFDM symbol, but they are changed from one symbol to another. Field measurements in big cities in Egypt show that in 2.5 GHz band, the power-delay profile of the channel is [9].

$$D(\tau_l) = C e^{-\tau_l/1.8 \cdot \tau_{rms}} \tag{5}$$

C is a constant. τ_{rms} is the root-mean-square value of the delay-spread of the reflections. The values of C and τ_{rms} depend on the building constructions and the Geography of the cities.

Under these assumptions, we can describe the system as a set of parallel Gaussian channels as shown in Fig. 2 with correlated attenuation H_m . The attenuation on each subcarrier is given by

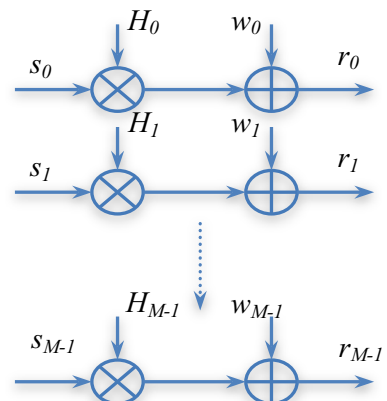
$$H_m = H \left(\frac{mf_s}{M} \right) \quad m = 0, 1, 2, \dots, M - 1 \tag{6}$$

$H(f)$ is the frequency response of the fading channel $h(t)$ during one HS-OFDM symbol and f_s is the sampling frequency of the system.

2.3 Received Signal Model

Synchronization is assumed between the received signal and the local subcarriers in the proposed receiver. If there is any error in the synchronization circuit, it is included in the delay parameter τ_{lm} as shown in Eq. (7c). Optimum synchronization algorithms are represented in [Paper under review 10]. They are based on ML criterion and are used to achieve synchronization in OFDM receivers. The HS-OFDM signal at the input of the receiver is represented by Eqs. (7a)–(7c)

Fig. 2 The Channel model of HS-OFDM system



$$r(t) = \int_{-\infty}^{\infty} s(\tau) \cdot h(t - \tau) \cdot d\tau + w(t) \tag{7a}$$

$$r(t) = \sum_{m=0}^{M-1} \sum_{k=0}^{K-1} \sum_{l=0}^{L-1} \alpha_{ml}(t) e^{j\phi_{ml}(t)} d_{mk} \int_{-\infty}^{\infty} p_m(\tau - kT) \cdot \delta(t - \tau_{lm} - \tau) \cdot d\tau + w(t) \tag{7b}$$

$$r(t) = \sum_{m=0}^{M-1} \sum_{k=0}^{K-1} \sum_{l=0}^{L-1} \alpha_{ml}(t) e^{j\phi_{ml}(t)} d_{mk} \cdot p_m(t - kT - \tau_{lm}) + w(t) \tag{7c}$$

$w(t)$ is a sample function of a white Gaussian noise process. The period of HS-OFDM symbol is smaller than the multipath delay-spread (T_m) of the channel. τ_{lm} is a uniform distributed random variable in the interval $[0, T_m]$. The integer, which is produced by dividing the delay τ_{lm} by the period of the HS-OFDM symbol, is equal to the number of the interfering symbols. The minimum number of the interfering symbols is one, however the maximum number is L . This is shown in Eq. (8).

$$1 \leq \left\lfloor \frac{\tau_{lm}}{T} + 1 \right\rfloor \leq L. \tag{8}$$

The HS-OFDM demodulator correlates the received HS-OFDM symbols with the M pulse-shape functions $p_m(t)$ of the used subcarriers. The i th-demodulated symbol of the n th-subcarrier is shown in Eq. (9b).

$$y_n(iT) = \int_0^T r(t) \cdot p_n(t - iT) \cdot dt \tag{9a}$$

$$y_n(iT) = \sum_{l=0}^{L-1} \sum_{m=0}^{M-1} \sum_{k=0}^{K-1} \alpha_{ml}(iT) e^{j\phi_{ml}(iT)} d_{mk} \rho_{mn}((i - k)T - \tau_{lm}) + z_n \tag{9b}$$

$\alpha_{ml}(iT)$ is a Rayleigh random variable. $\phi_{ml}(iT)$ is a uniform random variable. z_n is a Gaussian random variable with zero mean and σ_n^2 variance. ρ_{mn} is the correlation between the m th-subcarrier and the n th-subcarrier pulse shapes.

$$\rho_{mn}((i - k)T - \tau_{lm}) = \int_0^T p_m(t - \tau_{lm} - kT) \cdot p_n(t - iT) \cdot dt \tag{10}$$

$y_n(iT)$ is the complex coefficient of the n th-subcarrier at the i th symbol interval in the frequency domain. For ideal wireless channel (white channel), T_m is zero and the correlation coefficient in Eq. (10) is equal to:

$$\begin{aligned} \rho_{mn}((i - k)T) &= \int_0^T p_m(t - kT) \cdot p_n(t - iT) \cdot dt \\ &= \begin{cases} 1 & \text{if } i = k \\ 0 & \text{if } i \neq k \end{cases} \end{aligned} \tag{11}$$

For the model of the frequency-selective channel, which is shown in Eq. (4), the correlation coefficient ρ_{mn} is:

$$0 \leq \rho_{mn}((i - k)T - \tau_{lm}) \leq 1 \quad 0 \leq \tau_{lm} \leq T_m. \tag{12}$$

There are L preceding symbols, which affect the current symbol on each subcarrier. Consequently, the output signal of the n th correlator at the i th symbol period is reduced to:

$$y_n(iT) = \sum_{m=0}^{M-1} \sum_{k=i-L}^i \beta_{mk}((i - k)T) d_{mk} + z_n \quad 0 \leq n \leq M - 1 \tag{13a}$$

$$\beta_{mk}((i - k)T) = \sum_{l=0}^{L-1} \alpha_{lm}(iT) e^{j\phi_{lm}(iT)} \rho_{mn}((i - k)T - \tau_{lm}) \tag{13b}$$

$\beta_{mk}((i - k)T)$ is a complex Gaussian random variable. It represents the weight of the received k th symbol on the m th subcarrier, which interferes with the i th symbol on the n th subcarrier. The interfering signals in Eq. (13a) are divided according to their nature to three different interfering signals. The first is the ISI signal, the second is the ICI signal, and the third is the noise signal. The ICI signal is not only from the current symbols on the different non-orthogonal sub-carriers of the HS-OFDM symbol, but it is also from certain previous symbols on all non-orthogonal sub-carriers of the previous HS-OFDM symbols. Equation (14) shows the desired signal, the ISI signal, the ICI signal, and the noise signal at the output of the n th correlator.

$$\begin{aligned} y_n(iT) &= \sum_{m=0}^{M-1} \sum_{k=i-L}^i \beta_{mk}((i - k)T) d_{mk} + z_n \\ &= \beta_{ni}(0) d_{ni} + \sum_{k=i-L}^{i-1} \beta_{nk}((i - k)T) d_{nk} \\ &\quad + \sum_{m=0}^{M-1} \sum_{k=i-L}^i \beta_{mk}((i - k)T) d_{mk} + z_n. \\ &\quad m \neq n \end{aligned} \tag{14}$$

The first term represents the desired i th symbol on the n th subcarrier. It is affected by flat fading due to the time-varying nature of the wireless channel. The second term is the ISI signal from the symbols on the n th subcarrier. The third term is the ICI signal from the non-orthogonal subcarriers. The last term is the channel noise. In the next section, a design of a frequency-domain DFE is proposed in a new arrangement. This equalizer is used to eliminate the ISI signal and the portion of the ICI signal that is produced from the preceding symbols on the non-orthogonal sub-carriers. The equalizer is not able to eliminate all the ICI signals, because this needs to feed the equalizer with the current detected QAM symbols on each sub-carrier of the HS-OFDM symbol. This is not possible, because the QAM detector input is the equalizer output. The ICI signal from the current QAM symbols on the non-orthogonal subcarriers needs a separate technique to eliminate it, which is represented in Sect. 4.

3 Frequency Domain Decision Feedback Equalizer in a New Arrangement

In this section, a novel structure of a decision feedback equalizer is represented. The DFE equalizer is designed in the frequency domain, where it operates after the demodulator. Its input signal is the frequency domain signal shown in Eq. (15).

$$\begin{aligned}
 Y_n(i) = & \beta_{ni}(0)d_{ni} + \sum_{k=i-L}^{i-1} \beta_{nk}((i-k)T)d_{nk} \\
 & + \sum_{m=0}^{M-1} \sum_{k=i-L}^i \beta_{mk}((i-k)T)d_{mk} + z_n. \tag{15} \\
 & m \neq n
 \end{aligned}$$

The feedback path in the proposed equalizer is divided into two independent sections. The first feedback section minimizes the ISI from the previous detected symbols for each subcarrier. The second feedback section minimizes the ICI from the previous detected symbols on the other subcarriers of the HS-OFDM symbol. These two filters are built using adaptive LMS or RLS algorithms to continuously track the dynamic changes in the impulse response of the wireless channel.

Figure 3 shows the block diagram of the proposed DFE. The forward path of the DFE equalizer is designed to minimize the flat fading effect on the desired subcarrier signal.

3.1 Design of the Forward Filter

For each subcarrier, the forward filter is designed as one-tap adaptive filter. It compensates the effect of the complex gain of the channel on each subcarrier. The forward filter does not feed directly from the demodulator output as shown in Fig. 3. Feedback signals from feedback filters are subtracted first from the demodulator output, and then fed to the input of the forward filter. On the optimum operation condition of the DFE, the outputs of the feedback filters represent the ISI and ICI signals, which should be removed from the demodulator output before it is passed to the forward filter. This enhances the tracking capability of the forward filter, because the variance of the input interference signals is decreased [9]. The forward filter output is shown in Eq. (16). This signal represents the input to the QAM detector.

$$u_n(iT) = c_f \left(y_n(iT) - \widehat{ISI} - \widehat{ICI} \right) \tag{16}$$

c_f is the tap weight of the forward filter. \widehat{ISI} and \widehat{ICI} are the estimated values of ISI and ICI signals, respectively. The optimum design of c_f that minimize the mean square error between the detector output ($\hat{d}_n(iT)$) and input ($u_n(iT)$) is:

$$c_{of} = \hat{\beta}_{ni}^*(0). \tag{17}$$

3.2 Design of the ISI Feedback Filter

The ISI feedback filter is designed for each subcarrier. We assume that the subcarriers are orthogonal and no ICI is present. This assumption is for simplicity and to declare the idea

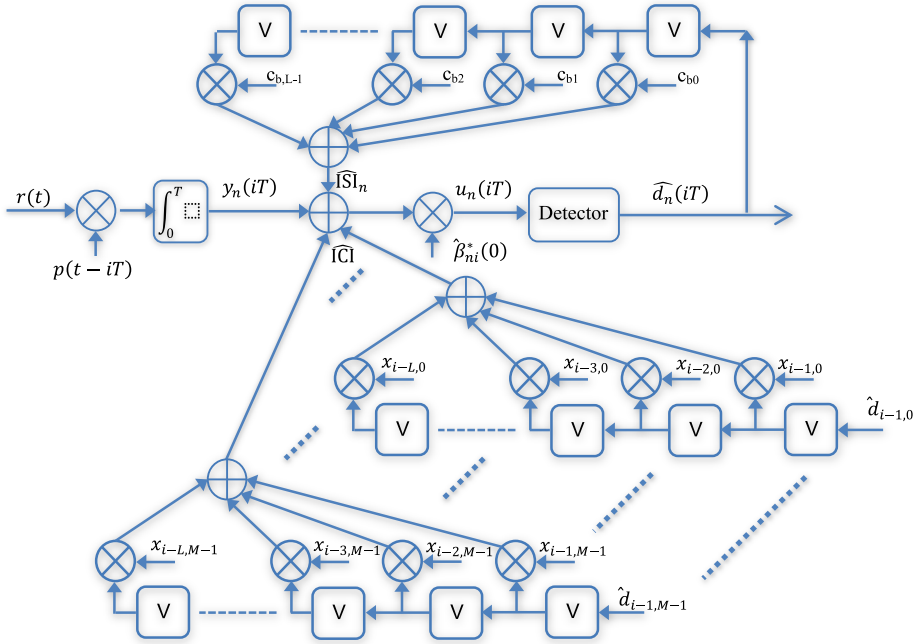


Fig. 3 The proposed receiver for HS-OFDM system

of the new proposed equalizer arrangement. In the next subsection, the general case of the existence of ISI and ICI signals is represented.

The analysis of the DFE is complex, because the design of the feedback filter is based on the error between the desired output of the filter and the estimated output [11]. The inputs of the feedback filter are the previous detected symbols. The feedback filter is designed to estimate the ISI_n signal from the previous interfering symbols of the n th subcarrier.

$$\widehat{ISI}_n = \mathbf{c}_b^H \cdot \mathbf{d}_n \tag{18}$$

\mathbf{d}_n is the input vector of the feedback filter of the n th subcarrier. It consists of the L previous symbols from $i-L$ to i . \mathbf{c}_b is the vector of the coefficients of the feedback filter. The length of the filter is equal to the number of the previous symbols that causes ISI_n . This number depends on the delay spread of the channel. It is equal to:

$$L_{FB} = \left\lceil \frac{T_m}{T} + 1 \right\rceil. \tag{19}$$

Theoretically, the estimation error between the desired response at the output of the feedback filter and the estimated response is equal to:

$$e_{FB} = ISI_n - \widehat{ISI}_n \tag{20}$$

Practically, this error cannot be measured directly. The ISI_n signal, which is the desired response of the feedback filter, cannot be separated and it is mixed with the desired symbol. This error can be calculated in an indirect way. The received signal consists of the desired

symbols plus ISI_n signal. The detector input is the difference between the received signal and the estimated ISI_n signal from the feedback filter. At optimum operation of the system and if the detector makes a correct decision of the current transmitted symbol, the error between the detector output and input is given by

$$\hat{d}_n - u_n = \hat{d}_n - \left((d_n + ISI_n) - \widehat{ISI}_n \right) = \widehat{ISI}_n - ISI_n. \tag{21}$$

Therefore, the error between the detector input and output is equal to the estimation error of the feedback filter. This is the parameter, which should be minimized. The optimum value of the feedback filter taps \mathbf{c}_{ob} , which minimizes the mean square value of the estimation error, will minimize the mean square value of the error between the detector input and output. This is the desired goal. The optimum solution for the coefficients vector of the feedback filter is given by

$$\mathbf{c}_{ob} = \mathbf{R}_b^{-1} \cdot \mathbf{p}_b \tag{22}$$

\mathbf{R}_b is the correlation matrix of the inputs of the feedback filter.

$$\mathbf{R}_b = \mathbf{E} \left[\hat{\mathbf{d}}_n \cdot \hat{\mathbf{d}}_n^T \right] = \sigma_d^2 \mathbf{I} \tag{23}$$

\mathbf{p}_b is the cross-correlation between the filter input and the desired output of the filter.

$$\mathbf{p}_b = \mathbf{E} \left[\hat{\mathbf{d}}_n \cdot \mathbf{ISI}_n^* \right] = \mathbf{E} \left[\hat{\mathbf{d}}_n \cdot \sum_{k=i-L}^{i-1} \hat{\beta}_{nk}^* ((i-k)T) d_{nk}^* \right] \tag{24}$$

$$\mathbf{c}_{ob} = \begin{bmatrix} \hat{\beta}_{n,i-1}^*(T) \\ \vdots \\ \hat{\beta}_{n,i-L}^*(LT) \end{bmatrix}. \tag{25}$$

3.3 Design of the Preceding ICI Feedback Filter

The same procedure, which is used to remove the ISI signal, can be used to remove the ICI signal from the previous symbols. The feedback filter that is used to remove the ICI consists of $(M-1)$ sub-filters. Each interfering subcarrier has its own tapped-delay-line filter, which is used to calculate the share of this interfering subcarrier in the total ICI signal. The input of the filter is the previous detected symbols on that subcarrier. The required outputs of all feedback filters are the estimated signals of the ISI and ICI. From Eq. (15), the ISI and ICI signals, which affect on the current symbol on the n th subcarrier, are:

$$I_n = \sum_{k=i-L}^{i-1} \beta_{nk} ((i-k)T) d_{nk} + \sum_{\substack{m=0 \\ m \neq n}}^{M-1} \sum_{k=i-L}^{i-1} \beta_{mk} ((i-k)T) d_{mk}. \tag{26}$$

According to the MMSE criterion, all feedback filters are designed to minimize the mean square error between the output of the filters and the desired response. The mean square value of the error is represented by:

$$E[|e|^2] = E \left[\left(I_n - \sum_{k=i-L}^{i-1} c_{bk} d_{kn} - \sum_{\substack{m=0 \\ m \neq n}}^{M-1} \sum_{k=i-L}^{i-1} x_{km} d_{km} \right)^2 \right]. \tag{27}$$

The problem is to choose the optimum value of the \mathbf{c}_b vector and \mathbf{x} matrix that represent the tap weights for the ISI removal filter and the group of the ICI removal sub-filters respectively. This is an optimization problem of two independent variables, because the ISI and ICI signals are two independent signals. The optimum value of c_{bk} is the value that makes the differentiation with respect to c_{bk} of the cost function in Eq. (27) equal to zero.

$$\begin{aligned} \frac{dE[|e|^2]}{dc_k} = E \left[-2 \left(\sum_{k=i-L}^{i-1} d_{nk} \right) \left(\sum_{k=i-L}^{i-1} \beta_{nk} ((i-k)T) d_{nk} \right. \right. \\ \left. \left. + \sum_{\substack{m=0 \\ m \neq n}}^{M-1} \sum_{k=i-L}^{i-1} \beta_{mk} ((i-k)T) d_{mk} \right) \right. \\ \left. + 2 \left(\sum_{k=i-L}^{i-1} d_{nk} \right) \left(\sum_{k=i-L}^{i-1} c_{bk}^* d_{nk} \right) \right. \\ \left. + 2 \left(\sum_{k=i-L}^{i-1} d_{kn} \right) \left(\sum_{\substack{m=0 \\ m \neq n}}^{M-1} \sum_{k=i-L}^{i-1} x_{km} d_{mk} \right) \right] = 0. \tag{28} \end{aligned}$$

The HS-OFDM symbols are produced from discrete memory-less source, so the data symbols on the different sub-carriers are statistically independent. The data symbols are assumed uniform random variable with zero mean (this is almost the real case), thus the data symbols on the different sub-carries are uncorrelated and the successive symbols on the same sub-carrier are uncorrelated too. Therefore, the following equation can be deduced.

$$E[d_{kn} \cdot d_{km}] = 0 \quad \Leftrightarrow \quad n \neq m \tag{29a}$$

$$E[d_{kn} \cdot d_{km}] = \sigma_d^2 \quad \Leftrightarrow \quad n = m \tag{29b}$$

$$E[d_{kn} \cdot d_{in}] = 0 \quad \Leftrightarrow \quad i \neq k. \tag{29c}$$

Using the previous facts on Eqs. (29a–29c) in Eq. (28), the result equation is:

$$-2\sigma_d^2 \sum_{k=i-L}^{i-1} \beta_{nk} ((i-k)T) + 2\sigma_d^2 \sum_{k=i-L}^{i-1} c_{bk}^* = 0. \tag{30}$$

This equation has infinite number of solutions for the filter taps c_{bk} one of these solutions is the solution shown in Eq. (25).

Now, we turn to calculate the optimum solution of x_{km} according to the MMSE criterion. This solution makes the derivative of the cost function in Eq. (27) with respect to of x_{km} equal to zero.

$$\begin{aligned} \frac{dE[|e|^2]}{dx_{km}} = E & \left[2 \begin{pmatrix} \sum_{m=0}^{M-1} \sum_{k=i-L}^{i-1} d_{mk} \\ m \neq n \end{pmatrix} \begin{pmatrix} \sum_{m=0}^{M-1} \sum_{k=i-L}^{i-1} x_{mk}^* d_{mk} \\ m \neq n \end{pmatrix} \right. \\ & - 2 \begin{pmatrix} \sum_{m=0}^{M-1} \sum_{k=i-L}^{i-1} d_{mk} \\ m \neq n \end{pmatrix} \left(\sum_{k=i-L}^{i-1} \beta_{nk}((i-k)T) d_{nk} \right. \\ & \left. \left. + \sum_{m=0}^{M-1} \sum_{k=i-L}^{i-1} \beta_{mk}((i-k)T) d_{mk} \right) \right. \\ & \left. + 2 \begin{pmatrix} \sum_{m=0}^{M-1} \sum_{k=i-L}^{i-1} d_{mk} \\ m \neq n \end{pmatrix} \begin{pmatrix} \sum_{k=i-L}^{i-1} c_{bk}^* d_{kn} \end{pmatrix} \right] = 0. \end{aligned} \tag{31}$$

By using the same facts in Eqs. (29a)–(29c), Eq. (31) will be:

$$2\sigma_d^2 \begin{pmatrix} \sum_{m=0}^{M-1} \sum_{k=i-L}^{i-1} x_{km}^* \\ m \neq n \end{pmatrix} - 2\sigma_d^2 \sum_{m=0}^{M-1} \sum_{k=i-L}^{i-1} \beta_{mk}((i-k)T) d_{mk} = 0 \tag{32}$$

This equation has infinite solutions for of x_{km} . One of these solutions is given in Eq. (33), where \mathbf{x}_{om} is the optimum tap-weight vector of the ICI DFE of the m th subcarrier.

$$\mathbf{x}_{om} = \begin{bmatrix} \beta_{m,i-1}^*(T) \\ \vdots \\ \beta_{m,i-L}^*(LT) \end{bmatrix}. \tag{33}$$

3.4 The Residual ISI and ICI Calculations

The optimum MMSE solution for the ISI and ICI feedback filters minimizes the effect of the interfering signals on the detected data, but it will not cancel them. There are residual

interfering signals that affect the detected symbols. The power of the residual interference signals represents the mean square value of the error between the actual ISI and ICI signals and the estimated ones at the output of the feedback filters.

Due to the fact that the ISI and ICI signals are uncorrelated and the mean of the estimation error on each signal is zero, the total mean square value of the residual interference signals is the sum of the individual mean square value of each residual interference signal as shown in Eq. (34).

$$E[(ISI_{residual} + ICI_{residual})^2] = E[(ISI_{residual})^2] + E[(ICI_{residual})^2]. \tag{34}$$

The minimum mean square value of the residual ISI signal equals the difference between the variance of the ISI signal and the variance of the estimated ISI signal produced by the ISI feedback filter as shown in Eq. (35a).

$$E[(ISI_{residual})^2] = \sigma_{ISI}^2 - \mathbf{p}_b^H \mathbf{R}_b^{-1} \mathbf{p}_b = \sigma_{ISI}^2 - \sum_l |\hat{\alpha}_{kl}|^2 \rho_{nm}^2 (-\hat{\tau}_{kl}) \sigma_{ISI}^2 \tag{35a}$$

$$\sigma_{ISI}^2 = \mathbf{c}_{ob}^H \cdot \mathbf{R}_b \cdot \mathbf{c}_{ob} \tag{35b}$$

By the same way, the minimum mean square value of the residual ICI signal equals the difference between the variance of the ICI signal and the variance of the estimated ICI signal produced by the ICI feedback sub-filters as shown in Eq. (36a).

$$E[(ICI_{residual})^2] = \sum_{m \neq n} \sigma_{ICI_m}^2 - \mathbf{p}_m^H \mathbf{R}_m^{-1} \mathbf{p}_m \tag{36a}$$

$$= \sum_{m \neq n} \left(\sigma_{ICI_m}^2 - \sum_l |\hat{\alpha}_{kl}|^2 \rho_{nm}^2 (-\hat{\tau}_{kl}) \sigma_{ICI_m}^2 \right)$$

$$\sigma_{ICI_m}^2 = \mathbf{x}_{om}^H \cdot \mathbf{R}_m \cdot \mathbf{x}_{om}. \tag{36b}$$

The residual interfering signals depend on the gains of the time-varying channel and the autocorrelation between the pulse-shape functions. The first dependence term can't be controlled because it depends on the natural of the channel. However, the second one, which is the autocorrelation between the pulse-shape functions, can be controlled. By choosing a suitable pulse shape, the autocorrelation function will rapidly decrease with the channel delays and this will reduce the ISI and ICI interference signals [12, 13].

4 ICI Cancellation of Current HS-OFDM Symbol

The receiver of the HS-OFDM system with M subcarriers contains M equalizers as the one shown in Fig. 3. Each subcarrier passes through its own equalizer. The equalizers reduce the ISI signal from the previous symbols on each subcarrier and the ICI signal from the previous symbols on the non-orthogonal subcarriers. The proposed equalizers also compensate the effects of the random gains of the channel, which affect the desired symbols. The ICI signal from the current symbols on the non-orthogonal subcarriers is not removed by the proposed feedback equalizers. The input signal to each detector of each subcarrier contains the desired QAM symbol plus the ICI signal, which comes from the current QAM symbols on the other non-orthogonal subcarriers. In addition, the detector input contains

the residual ISI and ICI signals from the previous symbols on each subcarrier plus noise. The residual ISI and ICI signals can be considered as a noise-like signal. They are added to the noise signal (z_n) to form a new noise signal (v_n). The variance of the new noise signal is equal to the variance of the channel noise plus the variance of the residual interfering signals. The input of the proposed detector of the n th subcarrier is:

$$u_n(iT) = \beta_{ni}(0)d_{ni} + \sum_{m \neq n} \beta_{mi}(0)d_{mi} + v_n \tag{37a}$$

$$v_n = R_{ISI} + R_{ICI} + z_n \tag{37b}$$

$$\begin{aligned} \text{var}(v_n) = & \sigma_{ISI}^2 - \sum_l |\hat{\alpha}_{kl}|^2 \rho_{nn}^2 (-\hat{\tau}_{kl}) \sigma_{ISI}^2 + (M - 1) \sigma_{ICI_m}^2 \\ & - \sum_{m \neq n} \sum_l |\hat{\alpha}_{kl}|^2 \rho_{nm}^2 (-\hat{\tau}_{kl}) \sigma_{ICI_m}^2 + \sigma_n^2. \end{aligned} \tag{37c}$$

The input signals to the M HS-OFDM detectors can be considered as M outputs of a demodulator of a multiuser system. Each subcarrier of the HS-OFDM system can be considered as a separate user in a multiuser system. Consequently, the multiuser detection techniques found in [14] can be used to eliminate the interference among the different subcarriers on the HS-OFDM system. In [14] there is a comparison between the Decorrelator and the MMSE multiuser detectors. These two detectors are suboptimum detectors but they are linear. The Decorrelator detector multiplies the input vector to the M HS-OFDM detectors with the inverse of the cross-correlation matrix between the different non-orthogonal subcarriers.

$$\mathbf{y}_d = \mathbf{R}^{-1}(\mathbf{u} + \mathbf{v}) \tag{38}$$

\mathbf{u} and \mathbf{v} are M -dimension column vectors that represent the vector of the input to the M HS-OFDM detectors and the vector of noise, respectively. \mathbf{R} is a $M \times M$ square matrix with elements ρ_{ij} , which represents the correlation coefficient between the i th and j th subcarriers. If the channel is not time varying the correlation coefficient ρ_{ij} is calculated as shown in Eq. (39).

$$\rho_{ij} = \frac{1}{2} \int_0^T (\cos(2\pi(f_i - f_j)t) + \cos(2\pi(f_i + f_j)t)) \cdot dt. \tag{39}$$

When the channel is time varying, the average value of the correlation coefficient is used to construct the correlation matrix \mathbf{R} . If there is a miss-synchronization between the received subcarriers and the local subcarriers, the correlation coefficient ρ_{ij} will be:

$$\rho_{ij} = \frac{1}{2} \int_0^T (\cos(2\pi(f_i - (f_j + f_e))t) + \cos(2\pi(f_i + (f_j + f_e))t)) \cdot dt. \tag{40}$$

The Decorrelator detector has the advantage of canceling the ICI signal if the optimum correlation matrix is calculated. In time varying channel, optimum calculation of the correlation matrix is difficult, thus there will be a residual ICI in the output of the detector. Moreover, the Decorrelator detector has the disadvantage of enhancing the background noise. For these reasons, a MMSE multiuser linear detector is used to optimize between the

ICI cancelation of the current symbols on the HS-OFDM subcarriers and the enhancement of the background noise.

The MMSE linear detector for the n th subcarrier chooses the vector \mathbf{w}_n that achieves:

$$\min_{\mathbf{w}_n} E \left[(d_n - \mathbf{w}_n^H \mathbf{u})^2 \right] \tag{41}$$

The MMSE linear transformation maximizes the signal to interference ratio at the output of the linear transformation. We can express this linear transformation as:

$$\mathbf{w}_n = \mathbf{w}_n^s + \mathbf{w}_n^o \tag{42}$$

where \mathbf{w}_n^s is spanned by the samples of the subcarriers pulse shapes $p_1(t), \dots, p_M(t)$ and \mathbf{w}_n^o is orthogonal to \mathbf{w}_n^s ; then

$$E \left[(d_n - \mathbf{w}_n^T \mathbf{u})^2 \right] = E \left[(d_n - \mathbf{w}_n^s \mathbf{u})^2 \right] + \sigma_v^2 \|\mathbf{w}_n^o \mathbf{u}\|^2. \tag{43}$$

Consequently, it is better to restrict attention to \mathbf{w}_n^s spanned by $p_1(t), \dots, p_M(t)$. This implies that the linear MMSE detector outputs a weighted combination of the M inputs of the M HS-OFDM detectors. Now we have M uncoupled optimization problems, which can be solved simultaneously by choosing the $M \times M$ matrix \mathbf{W} (whose columns is equal to \mathbf{w}_n^s) that achieves:

$$\min_{\mathbf{W} \in \mathbb{R}^{M \times M}} E \left[\|\mathbf{d} - \mathbf{W}^T \mathbf{u}\|^2 \right] \tag{44a}$$

$$\mathbf{u} = \mathbf{H} \mathbf{d} + \mathbf{v} \tag{44b}$$

\mathbf{H} is a $M \times M$ matrix and h_{ij} is given as:

$$h_{mn} = \beta_{mi}(0) = \sum_{l=0}^{L-1} \alpha_{lm}(iT) e^{j\phi_{lm}(iT)} \rho_{mn}(-\tau_{lm}). \tag{45}$$

The matrix \mathbf{H} is varied from symbol interval to another because the channel is time varying. Thus, continuous estimation of \mathbf{H} is required. The practical implementation of such a case is shown in [10]. By solving the optimization problem in (44a), the optimum solution of linear transformation matrix \mathbf{W} , which is used for cancelling the ICI between the non-orthogonal subcarriers of the HS-OFDM symbol, is given by Eq. (46).

$$\mathbf{W} = (\mathbf{H} + \sigma_v^2 \mathbf{I})^{-1}. \tag{46}$$

5 Implementation and Simulation Results

In this section, a comparison between a reference OFDM system and the proposed HS-OFDM system is represented using simulations and practical measurements. Long Term Evolution (LTE) is a 4th generation standard for cellular communications. LTE is based on OFDM modulation. It is used here as a reference OFDM system. The specifications of this reference model are shown in Table 1. The proposed HS-OFDM system uses the same channel bandwidth and the same maximum bit-rate as the reference OFDM system. However, the symbol rate of the proposed HS-OFDM is much bigger than the symbol rate

Table 1 The specifications of the reference and proposed OFDM systems

	Reference OFDM system	Proposed HS-OFDM system
Channel bandwidth	10 MHz	10 MHz
Symbol rate	15 K Symbols/s	500 K Symbols/s
Prefix length	4.69 μ s	–
Number of the subcarriers	667	20
Baseband modulation	16-QAM	16-QAM
Maximum bit-rate	40 Mbit/s	40 Mbit/s
Bandwidth efficiency	93.37%	100%

Table 2 The maximum delay-spread of wireless channel in Egypt

Environment	Maximum delay-spread	Maximum length of path difference
Suburban areas	50 ns–500 ns	15 m–150 m
Indoor for urbane areas		
Out doors in Urbane areas	1 μ s–6 μ s	300 m–1800 m

in the reference OFDM model. The proposed HS-OFDM system uses no cyclic prefix to increase the bandwidth efficiency. The number of the subcarriers in the proposed HS-OFDM is much smaller than the number of the subcarriers in the reference OFDM system. This reduces the power of the ICI signal in the proposed HS-OFDM system.

The used channel model in the simulations is the Rayleigh time-varying channel. The filed measurements of the delay-spread profile of this channel (in some urban and suburban areas in Egypt) are shown in Table 2. The maximum delay-spread in suburban environment is around 500 ns. The coherent bandwidth of the channel is approximately 2 MHz. It is greater than the sub-channel bandwidth but smaller than the total bandwidth of the OFDM signal. The frequency response of the channel is constant through the bandwidth of the sub-channel, but it varies through the total bandwidth of the OFDM signal. This coherent bandwidth causes no ISI on the sub-channel if cyclic prefix is used. However, there is ISI from one previous symbol in the proposed HS-OFDM system, because there is no cyclic prefix. On the other hand, the maximum delay-spread in the urbane environment is approximately 6 μ s. The coherent bandwidth of the channel is approximately 167 kHz. It is smaller than the sub-channel bandwidth in the proposed HS-OFDM system. The frequency response of the channel is not constant through the bandwidth of the sub-channel. This leads to strong ISI from at least 3 previous symbols in each sub-channel.

The simulations are done at two different frequency-errors (0.5% and 1%) between the received subcarriers and the local generated subcarriers. The source of the frequency-error may be the miss-synchronizations or the Doppler-frequency shift or both. The frequency-error is responsible for ICI between the used subcarriers. Figures 4a, b show the power of the interfering signal at each subcarrier in the proposed HS-OFDM system and the reference OFDM system. The total power of the ICI signals in the proposed HS-OFDM is -5.5 and 0.5 dB for frequency-errors of 0.5% and 1%, respectively. The average power of the ICI signal per subcarrier is -8.55 and -12.44 dB, for the same two frequency-errors respectively. In the reference OFDM system, the total power of the ICI signals is

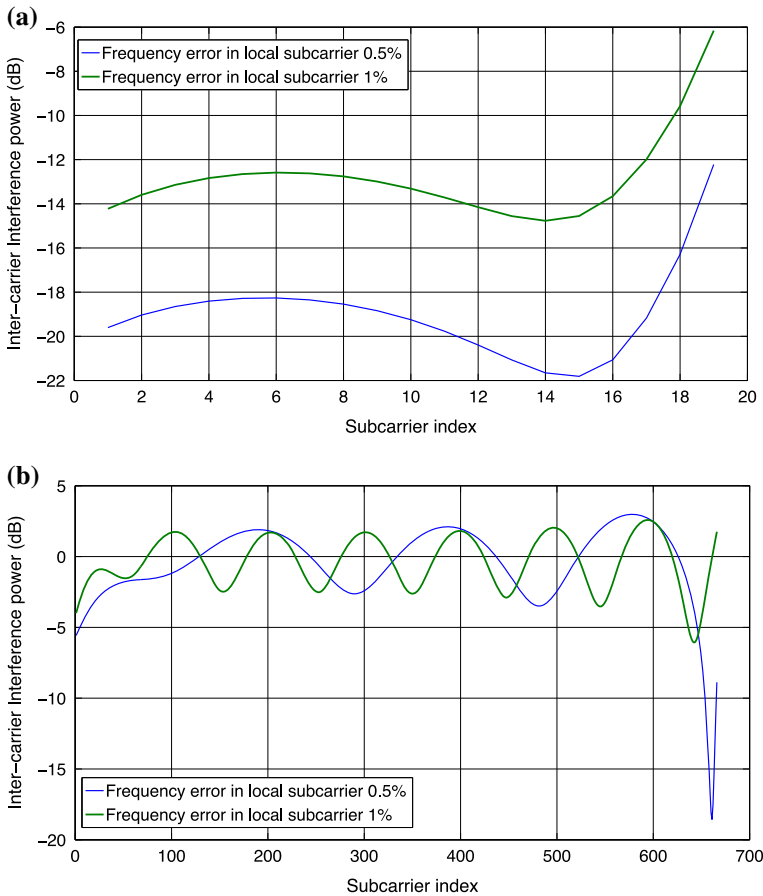


Fig. 4 **a** The ICI at each subcarrier in the proposed OFDM system. **b** The ICI at each subcarrier in the reference OFDM system

approximately 28 dB for both values of the used frequency-errors. The average power of ICI signal per subcarrier is 0 dB.

The power of the ICI signal in the reference OFDM model is the same for the used two values of the frequency-errors, because the power of the ICI signal is dominant with the number of the subcarriers instead of the value of the frequency-error at frequency-error greater than 0.3%.

Adaptive implementations of the proposed equalizers are shown here with the simulation results of its performance in the proposed HS-OFDM receiver. As we said before, the propose equalizers are implemented using adaptive algorithms to give the equalizers the ability of tracking the time variations in the wireless channel.

The proposed forward equalizer tracks the variations in the magnitude and the phase of the OFDM sub-channels. This filter has one-tap. The LMS implementation of this tap is shown in Eq. (47a).

$$c_f((i + 1)T) = c_f(iT) + \mu_f \cdot e_f \cdot u_n^*(iT) \tag{47a}$$

$$e_f = d_n(iT) - u_n(iT). \tag{47b}$$

The ISI feedback filter is designed according to the worst-case scenario of the outdoor environment. Using the data in Table 2, the filter length is calculated by Eq. (19).

$$L_{FB-ISI} = \left\lceil \frac{T_m}{T} + 1 \right\rceil = \left\lceil \frac{6\mu s}{2\mu s} + 1 \right\rceil = 4. \tag{48}$$

Therefore, the current symbol interferes with four previous symbols. The LMS adaptive implementation of the feedback ISI filter taps is shown in Eq. (49a).

$$c_b((i + 1)T) = c_b(iT) + \mu_{isi} \cdot e_{fb} \cdot \mathbf{d}_n^*(iT) \tag{49a}$$

$$e_{fb} = I_{ISI_n}(iT) - \widehat{ISI}_n(iT) \tag{49b}$$

$$I_{ISI_n}(iT) = y_n(iT) - \mathbf{x}^H(iT)\mathbf{d}(iT) - c_f^{-1}u_n(iT) \tag{49c}$$

I_{ISI_n} represents the ISI interfering signal on the n th subcarrier. $\mathbf{x}^H(iT)\mathbf{d}(iT)$ is the ICI component in the received signal $y_n(iT)$. During the training period, the filter is fed with a training sequence, which belongs to a signal space orthogonal on the signal space of the other sequences on the other subcarrier. Therefore, the filter tracks the ISI signal on its corresponding subcarrier.

The ICI feedback filter consists of a matrix of 4 rows and 19 columns. Each column represents the filter’s taps that are used to estimate the ICI share of its corresponding subcarrier. The ICI feedback filters’ taps are calculated using the adaptive LMS algorithm as shown in Eq. (50a).

$$\mathbf{x}_m((i + 1)T) = \mathbf{x}_m(iT) + \mu_{ici} \cdot e_m \cdot \mathbf{d}_m^*(iT) \tag{50a}$$

$$e_m = I_{ICI_m}(iT) - \widehat{ICI}_m(iT) \tag{50b}$$

$$I_{ICI_m}(iT) = y_m(iT) - \mathbf{c}_m^H(iT)\mathbf{d}_m(iT) - c_f^{-1}u_m(iT) \tag{50c}$$

I_{ICI_m} represents the ICI interfering signal on the m th subcarrier. $\mathbf{c}_m^H(iT)\mathbf{d}_m(iT)$ is the ISI component in the received signal $y_m(iT)$. \mathbf{x}_m is the taps vector of the m th feedback filter of the m th subcarrier. It represents the m th column in the \mathbf{x} matrix of the ICI equalizers. $\mathbf{d}_m^*(iT)$ is the data vector of the m th feedback filter of the m th subcarrier. It represents the m th column in the \mathbf{d} matrix of the ICI equalizers.

In the following simulation results, the average power of the desired subcarrier is 0 dB. Figures 5a, b show the average Bit-Error-Rate (BER) in the reference OFDM system and the proposed HS-OFDM system at the same simulation conditions. In Fig. 5a, the effect of the ISI signal is shown and the performance of its corresponding equalizer is evaluated at no ICI signal.

The power of the ISI signal before the proposed ISI equalizer is -27 dB. After the equalizer, the power of the residual ISI signal is around -55 dB. The used equalizer removes about 28 dB of the interfering signal. The power of the residual ISI signal is -55 dB. Figure 5a shows that the performance of the HS-OFDM with MMSE equalizer is better than the HS-OFDM with zero-forcing equalizer. With no ICI signal, the performance of the conventional OFDM system (reference system) is better than the performance of the

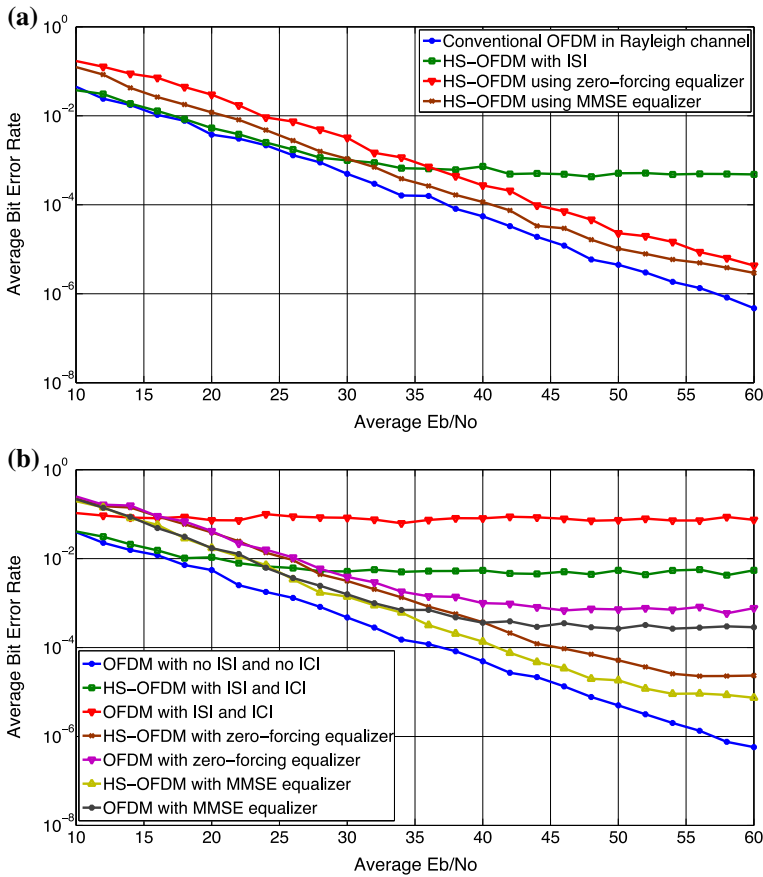


Fig. 5 **a** The average BER of the simulated systems with ISI and no ICI. **b** The average BER of the simulated systems with ISI and ICI

proposed HS-OFDM. However, the bandwidth efficiency of the proposed HS-OFDM system is 7% better than the bandwidth efficiency of the conventional OFDM system.

Once the ISI and the ICI signals exist, the performance of the conventional OFDM and HS-OFDM system gets worst as shown in Fig. 5b. The BER performance in the proposed HS-OFDM is better than the conventional OFDM, because the ICI signal in the proposed system is smaller than the ICI signal in the reference system. The average signal to interference ratio at the receiver input of the HS-OFDM system is 20 dB. However, the average signal to interference ratio at the receiver input of the reference OFDM system is approximately 7 dB. When the proposed receiver of the HS-OFDM system is used, the signal to interference ratio at the detector input will be 44 dB if zero-forcing criterion is used and 48.7 dB if MMSE criterion is used. The proposed equalizers remove about 24 dB to 28 dB from the interfering signal power. The residual interference power at the proposed equalizers output is -44 dB if zero-forcing criterion is used and -48.7 dB if MMSE criterion is used.

When the proposed equalizers are used with the reference OFDM system, the average signal to interference ratio at the detector input will be 28.2 dB if zero-forcing criterion is

used and 32.5 dB if MMSE criterion is used. The proposed equalizers are not able to enhance the performance of the proposed receiver as in the case of HS-OFDM model. Because, the power of the interfering signals in the reference OFDM system is much bigger than the power of the interfering signals in the proposed HS-OFDM system.

6 Conclusion

The paper gives a mathematical model of the OFDM signal in frequency-selective channel. This model is used to design a suitable receiver, which compensates the problems of the frequency-selective channel. According to the deduced mathematical model of the OFDM signal, a new high speed OFDM system is proposed. The symbol rate in the new system is bigger than the symbol rate in the conventional OFDM system. The proposed HS-OFDM has bandwidth efficiency 7% more than the conventional OFDM system. The ICI signal on the proposed HS-OFDM is much smaller than the ICI signal on the conventional OFDM system, because the number of the subcarriers in the proposed HS-OFDM system is smaller than the number of the subcarriers in the conventional OFDM. The performance of the adaptive multiuser algorithms, which are used to reduce the ICI signal in the proposed HS-OFDM, is better than conventional OFDM, because the ICI signal power in the proposed HS-OFDM is smaller. The proposed receiver for HS-OFDM can reduce the fading effects on each sub-channel, reduce the ISI from the previous symbols on each subcarrier, and the ICI signal from the non-orthogonal subcarriers.

References

1. Henkel, W., Taubock, G., Odling, P., Borjesson, P. O., & Petersson, N. (2002). The cyclic prefix of OFDM/DMT - An analysis. In *IEEE International Seminar on Broadband Communications*, Zurich, Feb. 2002.
2. Melsa, P. J. W., Younce, R. C., & Rohrs, C. E. (1996). Impulse response shortening for discrete multitone transceivers. *IEEE Transactions on Communications*, 44, 1662–1672.
3. Parsaee, G. R., Zamiri, H., & Khoshbin, H. (2004). Extended time domain SINR maximizing equalizer design for OFDM systems. In *Proceedings 14th Iranian Conference on Electrical Engineering ICEE 2004*, Vol. 1, Mashhad, Iran, pp. 249–254.
4. Zamiri-Jafarian, H., Parsaee, G. R., Khoshbin-Ghomash, H., & Pasupathy, S. (2004). SINR maximizing equalizer design for OFDM systems. In *Proceedings IEEE International Conference on Acoustic, Sound and Signal Processing*, 2004, Montreal, Canada.
5. Schuer, R. & Speidel, J. (2001). An effective equalization method to minimize delay spread in OFDM/DMT systems. In *IEEE Conference on Communications*, vol. 5, pp. 1481–1484, June 2001.
6. Chow, J., & Cioffi, J. M. (1992). A cost effective maximum likelihood receiver for multicarrier systems. In *Proceedings of International Conference on Communications*, Chicago, June 1992, pp. 948–952.
7. Zhu, J., Ser, W., & Nehorai, A. (2000). Channel equalization for DMT with insufficient cyclic prefix. In *Proceedings of IEEE 34th Asimolar Conference on Signals, Systems and Computers*, Vol. 2, Oct. 2000, pp. 951–955.
8. Yarali, A. (2004). MMSE-DFE equalizer design for OFDM systems with insufficient cyclic prefix. In *Proceedings of Vehicular Technology Conference*, 2004. VTC2004-Fall.
9. Hassan, A. Y. (2015). A wide band QAM receiver based on DFE to reject ISI in wireless time varying fading channel. *AEU - International Journal of Electronics and Communications*, 69(1), 332–343.
10. Paper under review.
11. Proakis, J. G. (2001). *Digital communications*. New York: McGraw-Hill Inc.
12. Hassan, A. Y. (2016). Digital modulation using complex-exponential basic functions and orthogonal pulse-shapes. *JÖKULL Journal (The Iceland Journal of Life Sciences)*, 66(2), 271–287.

13. Hassan, A. Y. (2016). Double rate OFDM system in time varying channel. In *Proceedings of The Twenty-First IEEE International Symposium on Computers and Communications (IEEE-ISCC2016)*, 2016.
14. Verdu, S. (1998). *Multuser detection* (1st ed.). Cambridge: Cambridge University Press.



Ashraf Y. Hassan received the B.Sc. degree (with honors) and the M.S. degree in electrical engineering from, Benha university, Benha, Egypt, in 2000 and 2004, respectively, and the Ph.D. degree in Electronics and Electrical Communications engineering from Cairo University, Cairo, in 2010. From 2000 to 2010, he served as a research and teaching assistant at the electrical technology department in Benha Faculty of Engineering. At 2010, he employed as an assistant professor in electronics and communication engineering in the electrical engineering department. He works nine years as a researcher in the research and development center in Egyptian Telephone Company from 2000 to 2009. From 2012 till now he works as a visitor assistant professor in Northern Border University – Faculty of Engineering, Saudi Arabia. His current research interests include detection and estimation theory, digital communication systems, modeling of time varying channels, interference cancellation techniques, signal processing, coding for high-data-rate wireless and digital communications and modem design for broadband systems.